A Novel Modular, Reconfigurable Battery Energy Storage System Design

Amir Farakhor
Department of Mechanical Engineering
University of Kansas
a.farakhor@ku.edu

Huazhen Fang
Department of Mechanical Engineering
University of Kansas
fang@ku.edu

***Abstract*—In this paper, a new modular, reconfigurable battery energy storage system is presented. The presented structure integrates power electronic converters with a switch-based reconfigurable array to build a smart battery energy storage system (SBESS). The proposed design can dynamically reconfigure the connection between the battery modules to connect a module in series/parallel or bypass a faulty module. The reconfigurability along with the use of the converters will bring a few important advantages, including better safety, robust power supply despite faults, variable voltage or power output, flexible individual control of battery modules, and balanced use of batteries. Further, the modular design allows to scale up to construct large-size SBESS. This work also elaborates the operation principles for the proposed SBESS design and illustrates its effectiveness through simulation study.**

***Index Terms*—Reconfigurable battery packs, DC-DC converters, energy management systems, energy storage systems (ESS), Lithium battery cells**

I. Introduction

Battery energy storage systems (BESS) have been widely used in various applications such as electrical vehicles, renewable energy integration, and portable devices. They are conventionally based on the hardwired series/parallel connection of battery cells. The cells are connected in series and parallel to provide the required voltage and capacity levels, respectively. This fixed, hardwired connection among battery cells leads to easy configuration and cost-effective solutions for the BESS development, but imposes various drawbacks as well. First, the BESS operation requires high safety, reliability and fault tolerance especially in safety-critical applications. With the fixed connection, the failure of just one cell will disrupt or shut down the operation of the BESS as a whole, and often, as a result, conservative operation must be enforced as a necessary trade-off for safety. Second, the fixed connection will make the BESS vulnerable to heterogeneity among the constituent cells. It is known that battery cells, even if manufactured in the same batch with the same electrochemistry, are still non-uniform in capacity and internal resistance. The different rates of degradation and aging in cycling operation may further drive up the heterogeneity. This issue will compromise the overall performance of the BESS. For instance, for a group of serially connected cells, the total capacity is limited by the weakest cell, and equalizers are often needed to overcome the problem [1], [2].

Recently, reconfigurable BESS (RBESS) have attracted much attention as a promising solution for the aforementioned issues. In [3], a battery switch array system has been proposed for aerospace applications. The proposed system offers dynamic and selective configuration of battery cells. However, the high number of switches is the main disadvantage of the proposed system. The study in [4] develops another reconfigurable battery switch array. Each battery cell needs six switches in this system which is costly, and requires a more complex control strategy. A reconfigurable battery system has also been studied in [5] to improve the reliability by bypassing the faulty cells. Similarly, the circuit design is not optimal which brings about higher power losses due to the high number of switches on the current flow path.

Meanwhile, power electronic converters have shown increasing promise to realize more advanced BESS [6]. A hybrid BESS has been presented in [7]. In this paper, DC-DC converters are employed for the cell equalization. However, the proposed system is still prone to faults due to the fact that the cells are connected in serial hardwired manner. In [8], DC-DC converters are connected with battery cells to enable independent control of them, which also allow to bypass and isolate faulty cells. However, the design is only limited to serial configuration of cells. An integrated reconfigurable converter topology has also been presented in [9]. The topology suffers from high power losses since there are a high number of ON-state semiconductors on the current flow path of the topology. The proposed structure in [1] is also a reconfigurable array which is connected to a DC-AC inverter. In this structure, cells currents are not regulated and contain fluctuations which can adversely affect cells' lifetime.

This paper is devoted to develop a modular, reconfigurable smart BESS (SBESS). Distinct from the existing studies, power electronic converters are integrated with a switch-based reconfigurable array. Here, the switch-based reconfigurable array dynamically modifies battery module connections, and DC-DC converters allow efficient and independent power processing control for the battery cells. With its unique circuit design, the presented SBESS benefits from various merits including robustness to cell faults, reliability, scalability, control flexibility, and cell balancing.

The rest of the paper is organized as follows. Section II will introduce the circuit design for the proposed SBESS.

In Section III, the performance characteristics of the SBESS will be discussed. Section IV will develop a control approach for the proposed SBESS. Section V will provide simulation results, and Section VI will conclude the paper.

II. Circuit Topology of the Proposed SBESS

This section presents the circuit structure design for the proposed SBESS. It begins with a switch-based circuit topology to enable reconfigurability. Then, power electronic converters are integrated into the topology to usher in new functions and achieve modularity.

A. Reconfigurability

The proposed reconfigurable circuit array is shown in Fig. 1(a). The circuit array consists of n cells and $3(n-1)$ switches. As is shown, each cell i, except the last one, is connected to its adjacent cell $i+1$ via three switches. The switch set associated with cell i is denoted as $\{S_{ij}\}$, where j is a switch's label within this set. There are three configuration modes for each cell in this structure. Adjacent cells (i and $i+1$) can be connected in series by turning ON the S_{i2} switch. Two cells will be in parallel via turning ON S_{i1} and S_{i3} switches. Furthermore, cell i will be bypassed/isolated by turning ON S_{i1}. Various cell configurations can be realized by the proper switching actions. To illustrate, a five-cell reconfigurable array is provided in Fig. 1(b). In this specific switch configuration, cells 1 and 2 are in series, while cells 4 and 5 are in parallel. In addition, cell 3 is bypassed from the array, assuming that it is failed or is unavailable for service. The current flow paths are also depicted in this figure.

The proposed reconfigurable structure will offer several important benefits. First, it can bypass and isolate cells subject to faults or failures, without shutting down the entire array. It is important to note that fault occurrence is not the only reason for cell isolation. Other safety measures can cause a cell to be bypassed such as excessive temperature rise. This function would provide a significant guarantee for the system-wide safety and reliability. Second, through reconfiguration, the array can reach various output voltage-capacity ratios to meet the needs arising in different power scenarios. Finally, compared to the literature, the design offers the most economic use of switches to allow arbitrary series/parallel configuration, to the best of our knowledge.

The above design crucially introduces switch-based reconfigurability. However, it is still limited in its ability to regulate or control the use of individual cells. As a result, the array may be unable to supply the needed voltage or power when a cell is switched off, or ensure cell balancing based on state of charge (SOC) of the modules. This motivates us to integrate converters into circuit array to further improve the design, as detailed below.

B. Power Electronic Converter Integration

The recent advancement in power electronics has led to DC-DC converters with high efficiency (up to 98%) and of compact size. Therefore, DC-DC converters have found increasing applications in battery management systems to enable cell equalization and other functions. To expand the design in Section II.A, power electronic converters can be integrated with battery cells to form an integrated battery module. Further, the integrated battery modules can be combined with the reconfigurable array shown in Fig. 1 to construct the whole circuit structure. This then leads to the structure of the proposed SBESS as shown in Fig. 2. The SBESS is comprised of n battery cells, n DC-DC converters, and $3(n-1)$ switches. In this paper, a bidirectional DC-DC converter is employed for battery cell integration. However, more sophisticated converters can also be used. Each bidirectional DC-DC converter also consists of two power switches, an inductor and a capacitor. The power will be delivered/received from input+ and output- ports.

A single module constituting the SBESS is also illustrated in Fig. 3. The bidirectional converter can process power in both directions so that the battery cell can be charged and discharged under controlled current, or power. It is worth mentioning that reconfigurability enables the system to change the connection of the integrated battery modules to obtain a wide range of output voltage-capacity ratios. For high output voltage levels, the modules can be configured in series, but the parallel configuration will be desirable for high power applications. The merits of the proposed SBESS system will be discussed thoroughly in the following section.

III. Discussion on Functions and Performance Characteristics

The proposed SBESS structure can provide various advantages through harnessing the combined strengths of modularity and reconfigurability. It is able to offer diverse functions as well as performance characteristics to meet different demands or criteria, which are discussed as follows.

A. Cell Balancing

In the proposed SBESS, the SOC balancing issue will mostly be alleviated. This is mainly because each battery cell is individually managed, and its charging/discharging power

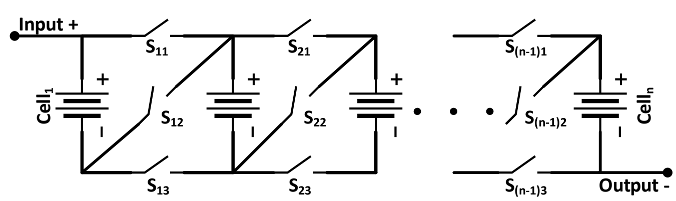

(a) The general circuit structure

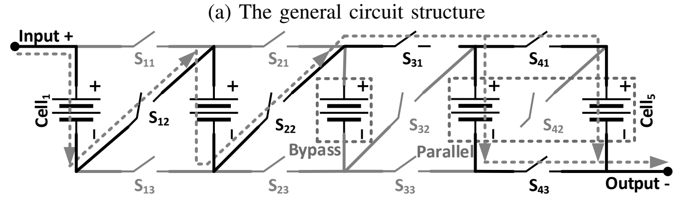

(b) Current flow paths of a 5-cell sample array

Fig. 1: The proposed reconfigurable array.

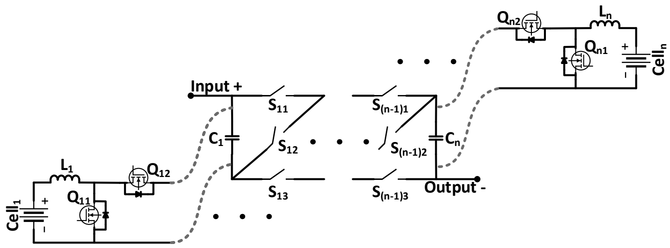

Fig. 2: The circuit structure of the proposed modular, reconfigurable SBESS.

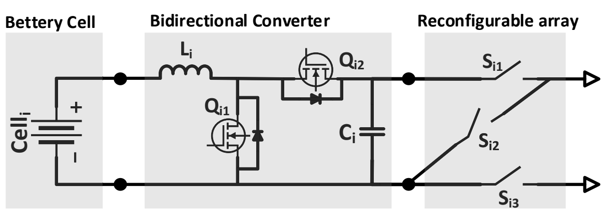

Fig. 3: A reconfigurable integrated battery module.

can be controlled via its corresponding DC-DC converter. The charging/discharging power of all cells can be controlled so that the SOC levels of all battery cells are equalized. Furthermore, SOC balancing can be performed concurrently along with charging/discharging. In the discharging cycle, battery cells with higher SOC levels will provide relatively more power to the load than the ones with lower SOC levels. On the other hand, battery cells with lower SOC levels will receive relatively more power in the charging cycle. The proposed SBESS structure does not require any additional or external power electronic devices for charging/discharging and cell equalization, and can perform both functions simultaneously.

To further inspect the cell balancing problem, one can formulate it as the question of how to allocate the total charging/discharging power among all battery cells so that the SOC levels of all battery cells will be equalized within a specific time horizon. According to the law of conservation of power, the following equation can be written:

$$P_{\text{total}} = \sum_{i=1}^{m} P_i, \tag{1}$$

where m is the number of available cells (some cells might be bypassed and isolated due to faults in the cells), and P_i is the power of battery cell i. The power ratio of cell i to cell j can be defined according to their SOC levels as follows:

$$\frac{P_i}{P_j} = \begin{cases} (\frac{\text{SOC}_i}{\text{SOC}_j})^k, & \text{Discharging mode} \\ \\ (\frac{\text{SOC}_j}{\text{SOC}_i})^k, & \text{Charging mode} \end{cases}, \tag{2}$$

where k is a positive real number which can be selected to tune how much power cell i should supply or receive relative to cell j. Smaller values for k mean that the SOC balancing among cells will take a longer time, and larger values for k will increase the speed of the SOC balancing. The selection of k must also take into consideration the limit of the charging/discharging power that a cell allows. If there are m number of available cells, there will be $m-1$ equations based on (2) to quantify relative power allocation, and along with (1), the power of all available cells can be calculated.

B. Power Rating and Voltage Stress

Since the semiconductors can only withstand specific maximum voltage and current stresses, this subsection is devoted to study the voltage and current stresses of the semiconductors employed in the proposed SBESS. The reconfigurable array, as shown in Fig. 1(a), consists of $3(n-1)$ power switches. The current stresses of these power switches can be expressed as:

$$i_{S_{i1}}^{\max} = i_{S_{i2}}^{\max} = i_{S_{i3}}^{\max} = \max\{i_{\text{load}}^{\max}, i_{\text{charge}}^{\max}\}, \tag{3}$$

where $i_{\text{load}}^{\max}$ and $i_{\text{charge}}^{\max}$ are the maximum discharging and charging currents, respectively. Considering Fig. 3, the voltage stresses can also be determined as below:

$$v_{S_{i1}}^{\max} = v_{S_{i2}}^{\max} = v_{S_{i3}}^{\max} = v_{C_i}^{\max}, \tag{4}$$

where v_{C_i} is the output capacitor voltage of the i^{th} DC-DC converter. The output capacitor voltage of the conventional bidirectional DC-DC converter can ideally be expressed as:

$$v_{C_i} = \frac{1}{1-D_i} V_{\text{cell}_i}, \tag{5}$$

where V_{cell_i} is the terminal voltage of the i^{th} battery cell, and D_i is the duty cycle of the switch Q_{i1} in the corresponding DC-DC converter.

As it can be seen from Fig. 3, the battery cell is connected to an inductor in the input stage of the DC-DC converter. This allows a proper control on the current flowing through the battery cell by the DC-DC converter. The current ripple across the battery cell current can be expressed as:

$$\Delta i_{L_i} = \frac{D_i V_{\text{cell}_i}}{L_i f_s}, \tag{6}$$

where L_i, D_i, and f_s are the inductance, duty cycle of the switch Q_{i1}, and the switching frequency, respectively. Higher switching frequency results in a lower current ripple which allows smaller inductor sizes. As the compactness of the SBESS is important, it is favorable to select higher switching frequency levels for the DC-DC converters.

The number of ON power switches in the current flow path is an important criterion in the efficient operation of the switching systems. As the reconfigurable array will not be switched fast, it can be considered that the switching losses across the power switches can be neglected, and the conduction losses are dominant. Therefore, it is desirable to minimize the number of ON-state power switches in the current flow path. In the reconfigurable array shown in Fig. 1, there is only a single power switch in the current flow path in the series and bypass configuration modes. On the other hand, there will be two power switches in the current flow path in the parallel configurations. However, it should be considered that the current will be divided between two switches in this case resulting in a lower current for each switch. As a result, the proposed reconfigurable array can achieve very high efficiency levels by employing power switches with ultra-low ON-state resistance. This is possible since the voltage stresses of the power switches are very low in the proposed structure.

It can be concluded that the voltage stresses of the power switches in the DC-DC converters (Q_{i1} and Q_{i2}) are the same as the voltage stresses of the power switches in the reconfigurable array (4). Moreover, the current stresses of these power switches ($i_{Q_{i1}}^{\max}$ and $i_{Q_{i2}}^{\max}$) are the maximum battery cell current ($i_{\mathrm{cell}_i}^{\max}$).

C. Fault Tolerance and Reliability

Operational safety and reliability are essential for the use of lithium-ion battery systems in high-stakes, safety-critical applications across the transportation, grid, aerospace and military sectors. This fact serves as a main motivation for the proposed SBESS, which, by design, offers the promise of being safer and more reliable.

This merit comes from the capability of reconfigurability which makes the isolation of faulty components possible in the system. Power electronic converters also make the faults tolerable with the output voltage regulation capability. It is also important to note that as each battery cell is connected to a power electronic converter, the failure in each one of them will result in the isolation of the cell from the array. In other words, possible failures in the DC-DC converters are tolerable as well.

Another important characteristic of the proposed SBESS is its output voltage regulation capability in its discharging mode. When a fault occurs to a battery cell, the faulty battery cell will be bypassed and isolated from the array. If no measures are to be taken, the total output voltage of the array will reduce. However, with the integration and control of DC-DC converters, the output voltage can be regulated to immediately recover from the effect due to the bypass of the faulty cell. This means that the SBESS will maintain its pre-specified reference output voltage.

D. Further Discussions

The proposed SBESS design can also deliver some other functions and advantages beyond the reach of conventional battery systems. An example in case is that a conventional BESS requires to use battery cells of the same type and produced by the same manufacturer. The main reason for identical battery cells is to mitigate the degradation and aging mismatches among battery cells. However, the proposed system would obviate such a need, to the benefit of some practical applications. Different types of battery cells can be utilized in a single SBESS which improves the versatility of the proposed system.

It has already been mentioned in Section III.A that the SBESS can guarantee balanced SOC levels of battery cells. Further, it can be exploited to enable temperature balancing among the cells through thermal-aware power allocation. Specifically, one can design appropriate power distribution methods to dynamically regulate the temperature among cells, which will allow the SBESS to operate more safely.

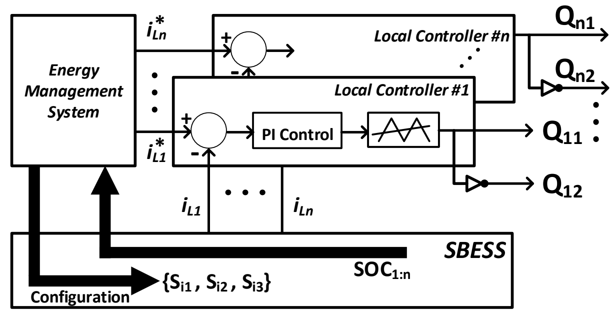

Fig. 4: The proposed hierarchical control strategy.

IV. Presented Control Approach

To take full advantage of the proposed SBESS, it is vital to design competent control strategies. Control design, however, is non-trivial. First, different functions may require different ways or at least involve different considerations to control the system. Second, the overall control space of the SBESS is very large due to the mixed use of switches and converters, making it formidable to find out optimal control methods. Finally, the SBESS may have complicated underlying dynamics as a result of the many constituent cells. All the difficulty yet presents exciting research challenges, which will be pursued in our future work. Here, to validate and demonstrate the benefits of the SBESS, a specific control task is investigated.

To overcome the complexity of the SBESS in structure, the study develops a hierarchical control strategy, which builds upon the notion of dividing the control responsibilities into different layers. Fig. 4 shows the overall control diagram. The control strategy has two layers. The top layer, named energy management system (EMS), is responsible to control the operation mode (topological configuration for the switches S_{ij}, and power allocation) of the SBESS. At the bottom layer is local controllers, which are meant to control the DC-DC converters.

Local controllers will be in charge of power electronic converters to manage the power switches of the converters. The main goal of the local controllers is to ensure that the actual cell current values track the corresponding reference values, which are provided by the EMS. Various types of controllers can be employed to control the DC-DC converters. In this paper, proportional-integral (PI) controllers are utilized as indicated in Fig. 4.

The EMS itself runs a two-step procedure. The first step is to solve an optimization problem about the optimal topological configuration for the SBESS. In other words, the EMS is tasked to find out a sufficient or even optimal topological configuration of the SBESS. The optimization problem must be designed to take into account the bypass/isolation of faulty cells and the configuration modes (series or parallel) of the other available cells. The second step calculates the reference discharge/charge currents of each cell. This step will account for the SOC of the cells such that the current assigned for a cell is commensurate with its SOC level to improve the SOC balance. Consider the EMS design, an optimization problem to find out the optimal configuration of the SBESS can be formulated as follows:

$$\begin{aligned} \min_{\xi} \quad & \lambda_0 \beta + \lambda_1 b J_0 + \lambda_2 (v_{\text{out}} - v_{\text{out}}^*)^2 + \lambda_3 (C_{\text{out}} - C_{\text{out}}^*)^2, \\ \text{s.t.} \quad & P_{\text{total}} = \sum_{i=1}^{m} P_i, \\ & i_{L_i} \le i_{L_i}^{\max} \quad i = 1, 2, ..., m, \end{aligned} \tag{7}$$

where ξ is the configuration of the battery cells which indicates the status of the switches $S_{i1:3}$. Also, λ_i for $i = 0, 1, 2, 3$ are the weighing factors for the optimization problem. Furthermore, m is the number of available cells. $i_{L_i}^{\max}$ is the maximum charge/discharge current of cell i; β is the reconfiguration cost, which is introduced to reduce the number or frequency of reconfigurations over time. It is usually undesirable to change the configuration of the SBESS unless there is a need. The reconfiguration cost β can be easily calculated by comparing the configuration variable ξ in time steps k and $k-1$.

In addition, J_0 is the cost of bypassing an active battery cell. If a battery cell is not faulty, it is desired that the cell contributes to the system. J_0 is a constant positive real value and b is the number of bypassed active battery cells.

The output voltage of the SBESS (v_{out}) can be determined by the output voltage of the DC-DC converters (v_{C_i}) and the configuration variable ξ. For instance, if all the battery cells are connected in series, the output voltage will simply be the total sum of v_{C_i} for all i. Similarly, the total capacity (C_{out}) can be calculated according to the configuration variable ξ and the capacity of each battery cell. If all the cells are configured in parallel, the total capacity will be the sum of all cells' capacities.

The above optimization problem would resist closed-form solution, but numerical solution based on mixed integer programming can come to help. It is important to note that the battery dynamics, such as output voltage and SOC of battery cells, are slow (not as fast as power electronic converters), so the EMS can be run in larger time intervals, and once the fault detection system identifies a malfunction. Therefore, the computational load can be easily handled.

When the SBESS is relatively small in size, the brute-force enumeration approach will be adequate, which is also considered in the simulation in Section V. This method will just enumerate all possible configurations for the SBESS. Then, all generated cases can be assessed by the predefined objective function (7). The objective function will ensure the isolation of faulty cells from the array and the output voltage regulation. To accelerate the enumeration process, any case will be discarded immediately once seeing violation of this objective. For instance, if a case attempts to utilize a faulty cell (direct violation), the path will be considered as invalid and will not be continued anymore. After the configuration is determined, the load allocation can be done according to (2).

V. Simulation Results

Based on the control design in Section IV, this section presents a simulation study. A four-cell SBESS is considered with the Samsung INR18650-25R battery cells. The cells are represented by the well-known Thevenin model in the simulation, and the identification of the model from experimental data is discussed in [10]. The parameter specification of the simulated model is given in Table I. Output voltage and power reference values are considered to be 19.5 V and 40 W. There are initially no faults in the system. To highlight the effective cell balancing, the initial SOC of the battery cells is selected as 0.9, 0.8, 0.7, and 0.6. The obtained simulation results are shown in Fig. 5-8.

TABLE I: The parameter specification of the SBESS.

Specifications	Values
Battery cell capacity	2,500 mAh
Cell nominal voltage	3.6 V
Discharge cut-off voltage	2.5 V
Inductor (L), ESR	33 μH, 0.2 Ω
Capacitor (C)	10 μF
Switching frequency	250 kHz

The output voltage (v_{out}) of the SBESS is depicted in Fig. 5. As it can be seen, the output voltage of the SBESS is regulated to track the reference of 19.5 V. At time instant $t = 0.1$ s, a fault occurs to cell 3, and it is bypassed and isolated by EMS. Although the output voltage suffers a drop due to the fault in the system, the control strategy immediately isolates cell 3 from the array, and the converters are controlled to recover the voltage soon by increasing the power level of the remaining active cells.

The current profiles of all the cells along with the output voltages of DC-DC converters are shown in Fig. 6. It is seen that, cell 1 with the relatively higher SOC level provides more power to the system in comparison with the other lower-SOC cells. In the same manner, cell 4 delivers the least power because of its lowest SOC. At time instant $t = 0.1$ s, when

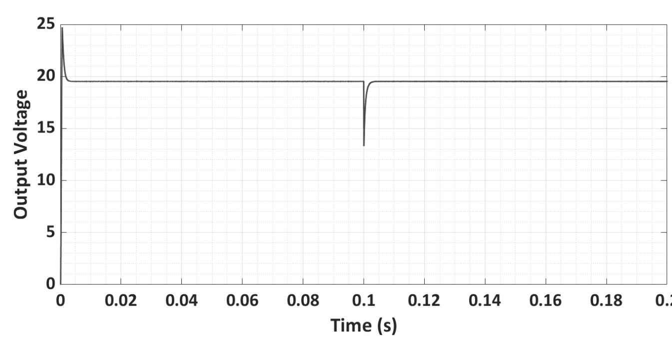

Fig. 5: The total output voltage of the SBESS.

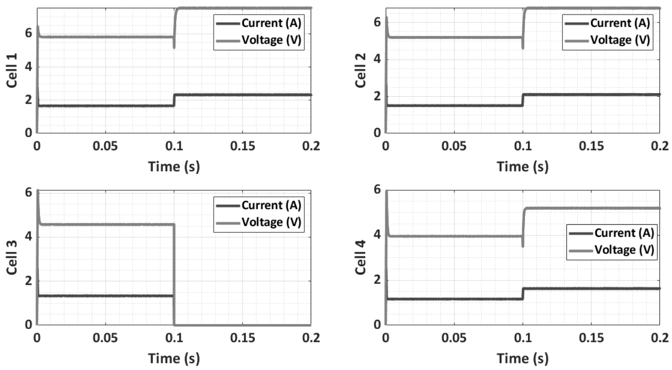

Fig. 6: The output voltages of DC-DC converters, and currents of battery cells.

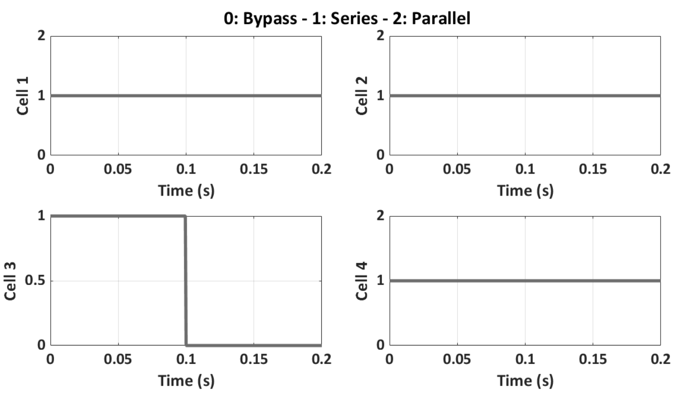

Fig. 7: The configuration of the battery cells.

cell 3 is bypassed and isolated, the remaining cells are all regulated to provide more power to compensate for the voltage loss and regulate the output voltage level. Fig. 7 shows the configuration of each cell within the simulation horizon the simulation horizon, in which "1" represents series connection and "0" stands for bypass.

It is also worth noting that, although the nominal voltage of each cell is 3.6 V, the DC-DC converters boost the cell voltages with flexibility so that the output voltage meets the necessary requirements. Fig. 8 shows the discharge rates of battery cells. Discharge rates are calculated by the SOC derivative with respect to time. As it can be seen, cell 1 with the highest SOC level discharges faster than other remaining cells. This results from the proper power allocation of the EMS which guarantees the SOC balancing. Overall, the simulation results validate the capability of the SBESS in providing key functions of fault tolerance, SOC balancing, and output voltage regulation.

VI. Conclusions

As lithium-ion batteries have become the technology of choice for energy storage in many sectors, there is a growing need for battery system design to ensure safety, reliability and powering flexibility. To meet this need, this paper proposes the SBESS design. Differing from the literature, the design features an integration of switches and DC-DC converters with

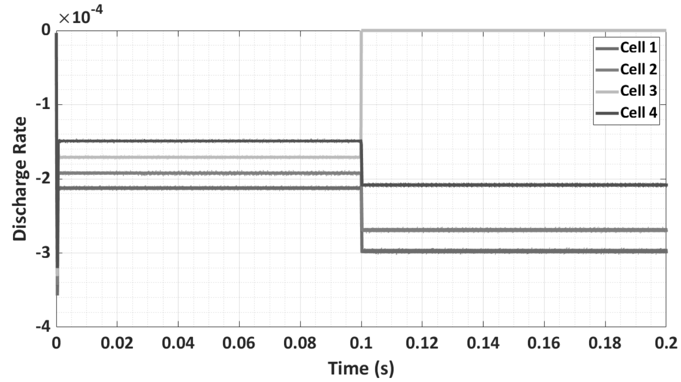

Fig. 8: The discharge rates of the battery cells.

the battery cells, where the switches offer reconfigurability for cell connection, and the converters provide modularity while allowing efficient power conversion for the cells. Many advantageous functions result from the proposed design, which, among others, include safety based on bypass of faulty or risky cells and fault-tolerant power supply. The study also develops a hierarchical control strategy for the proposed SBESS and validates it through simulation. The proposed SBESS can find promising use in many high-stakes applications.

References

[1] O. Salari, K. H. Zaad, A. Bakhshai, and P. Jain, "Reconfigurable hybrid energy storage system for an electric vehicle DC–AC inverter," *IEEE Transactions on Power Electronics*, vol. 35, no. 12, pp. 12 846–12 860, 2020.

[2] Q. Ouyang, J. Chen, J. Zheng, and H. Fang, "Optimal cell-to-cell balancing topology design for serially connected lithium-ion battery packs," *IEEE Transactions on Sustainable Energy*, vol. 9, no. 1, pp. 350–360, 2018.

[3] M. Alahmad, H. Hess, M. Mojarradi, W. West, and J. Whitacre, "Battery switch array system with application for jpl's rechargeable micro-scale batteries," *Journal of Power Sources*, vol. 177, no. 2, pp. 566–578, 2008.

[4] S. Ci, J. Zhang, H. Sharif, and M. Alahmad, "Dynamic reconfigurable multi-cell battery: A novel approach to improve battery performance," in *2012 Twenty-Seventh Annual IEEE Applied Power Electronics Conference and Exposition (APEC)*, 2012, pp. 439–442.

[5] F. Jin and K. G. Shin, "Pack sizing and reconfiguration for management of large-scale batteries," in *2012 IEEE/ACM Third International Conference on Cyber-Physical Systems*, 2012, pp. 138–147.

[6] B. Dong, Y. Li, and Y. Han, "Parallel architecture for battery charge equalization," *IEEE Transactions on Power Electronics*, vol. 30, no. 9, pp. 4906–4913, 2015.

[7] R. de Castro, C. Pinto, J. Varela Barreras, R. E. Araújo, and D. A. Howey, "Smart and hybrid balancing system: Design, modeling, and experimental demonstration," *IEEE Transactions on Vehicular Technology*, vol. 68, no. 12, pp. 11 449–11 461, 2019.

[8] Y. Li and Y. Han, "A module-integrated distributed battery energy storage and management system," *IEEE Transactions on Power Electronics*, vol. 31, no. 12, pp. 8260–8270, 2016.

[9] M. Momayyezan, B. Hredzak, and V. G. Agelidis, "Integrated reconfigurable converter topology for high-voltage battery systems," *IEEE Transactions on Power Electronics*, vol. 31, no. 3, pp. 1968–1979, 2016.

[10] N. Tian, Y. Wang, J. Chen, and H. Fang, "One-shot parameter identification of the Thevenin's model for batteries: Methods and validation," *Journal of Energy Storage*, vol. 29, p. 101282, 2020.